JPET Fast Forward. Published on February 14, 2017 as DOI: 10.1124/jpet.116.237255
This article has not been copyedited and formatted. The final version may differ from this version.

Label-free dynamic mass redistribution reveals low density, pro-survival α_{1B}-adrenergic receptors in human SW480 colon carcinoma cells

Dorathy-Ann Harris, Ji-Min Park, Kyung-Soon Lee, Cong Xu, Nephi Stella and Chris Hague

Author affiliations:

Department of Pharmacology (D.-A.H., J.-M.P., K-S.L., C.X., N.S., C.H.); and Department of Psychiatry and Behavioral Sciences (C.X., N.S.), University of Washington School of Medicine, Seattle, Washington.

Running Title: Pro-survival α_{1B}-ARs in SW480 colon carcinoma cells

Address correspondence to:

Dr. Chris Hague Ph.D., Department of Pharmacology, University of Washington School of Medicine, 1959 Pacific St, HSB-D430/431, Box 357280, Seattle, Washington, USA.

E-mail: chague@uw.edu

Phone: 206-221-4612

Fax: 206-685-3822

Number of text pages: 28

Number of tables: 2

Number of figures: 7

Number of references: 59

Number of words in

Abstract: 147

Introduction: 464

Discussion: 900

Abbreviations:

AR, adrenergic receptor; DMR, dynamic mass redistribution; GPCR, G protein-coupled receptor; ISO, isoproterenol; NE, norepinephrine; pA_2, affinity constant; PHE, phenylephrine.

JPET Fast Forward. Published on February 14, 2017 as DOI: 10.1124/jpet.116.237255
This article has not been copyedited and formatted. The final version may differ from this version.

Abstract

Small molecules that target the adrenergic family of G protein-coupled receptors (GPCRs) show promising therapeutic efficacy for the treatment of various cancers. Herein, we report that human colon cancer cell line SW480 expresses low-density functional α_{1B}-adrenergic receptors (ARs) as revealed by label-free dynamic mass redistribution (DMR) signaling technology and confirmed by quantitative reverse-transcriptase polymerase chain reaction analysis. Remarkably, while endogenous α_{1B}-ARs are not detectable via either [^{3}H]-prazosin binding analysis or phosphoinositol hydrolysis assays, their activation leads to robust DMR and enhanced cell viability. We provide pharmacological evidence that stimulation of α_{1B}-ARs enhances SW480 cell viability without affecting proliferation, whereas stimulating β-ARs diminishes both viability and proliferation of SW480 cells. Our study illustrates the power of label-free DMR technology for identifying and characterizing low-density GPCRs in cells and suggests that drugs targeting both α_{1B}- and β-ARs may represent valuable small molecule therapeutics for the treatment of colon cancer.

Introduction

Catecholamines play a key role in regulating multiple physiological responses, with the overarching goal of enhancing organism survival. However, in certain instances, prolonged catecholamine exposure produces detrimental effects on target organs that lead to cardiovascular disease (e.g. congestive heart failure, hypertension, cardiac arrhythmias and renal failure) and/or psychiatric disorders (e.g. post-traumatic stress disorder and hyperactivity disorders). Although the molecular mechanisms that mediate these detrimental effects remain to be fully understood, it is well appreciated that chronic adrenergic receptor (AR) activation ultimately leads to deleterious alterations in cell morphology (Lefkowitz et al, 2000; O'Connell et al, 2006; Catapano et al, 2007).

Recent evidence suggests that catecholamine signaling may also play a role in cancer pathogenesis. Specifically, chronic β-AR activation drives primary tumor growth and metastasis by increasing the production of angiogenetic factors, enhancing invasion of cancer cells through the stimulation of matrix-metalloproteinase dependent-migration, and/or affecting cancer cell viability and resistance to apoptosis (reviewed in Cole et al, 2011). As such, non-selective β-AR antagonists improve clinical outcomes of human cancer patients, and single-nucleotide polymorphisms in the β-ARs (or its signaling effectors) influence disease outcome (reviewed in Perez-Sayans et al, 2010). These studies suggest that among the molecular mechanisms involved in catecholamine signaling, β-ARs represent a promising target to treat cancer.

The effect of chronic activation of α_1-ARs on cancer pathogenesis and prognosis remains poorly understood. Quinazoline-based α_1-AR antagonists doxazosin and terazosin can induce tumor cell apoptosis (Anglin et al, 2002; Partin et al, 2003), although it remains unclear if these effects occur through α_1-AR and/or non-α_1-ARs dependent mechanisms (reviewed in Kyprianou et al, 2009). This question is particularly relevant when considering the three known subtypes of α_1-AR (α_{1A}, α_{1B}. α_{1D}) and their differential coupling in various cell types. For example, in murine

models, chronic activation of α_{1A}-ARs reduces cancer incidence and prolongs lifespan, whereas chronic α_{1B}-AR activation typically produces deleterious effects on multiple organ systems (Collette et al, 2014; Wang et al, 2000; Zuscik et al, 2000; Papay et al, 2002; Doze et al, 2009). As such, understanding the effects of chronic α_1-AR activation in specific cancer subtypes is essential.

Our laboratory studies macromolecular complexes formed by distinct α_1-AR subtypes and how complex architecture influences α_1-AR signaling and physiological function. We recently showed that α_1-AR subtypes associate with selective intracellular molecular scaffolds that dictate their pharmacodynamic and signaling characteristics (Camp et al, 2015; Lyssand et al, 2010; Lyssand et al, 2008). Interestingly, proteomic screening indicates cell-type specific α_1-AR:PDZ-protein complexes are formed in human SW480 colon cancer cells, suggesting α_1-ARs may couple to non-canonical, G-protein independent signal transduction mechanisms in this cell line (Camp et al, 2015). Thus, we used label-free dynamic mass redistribution assays to pharmacologically identify endogenous α_1-AR subtypes functionally expressed in SW480 colon carcinoma cells, thereby facilitating their examination as potential anti-neoplastic drug targets.

Materials and Methods

Reagents and plasmids

Human α_{1B}-AR cDNAs were subcloned in pSNAPf (New England Biolabs) using In-Fusion HD cloning technology (Clontech) as described in (Kountz et al, 2016). 5-methylurapidil (U101), BMY 7378 HCl (B134), clonidine HCl (C7897), (±) cyclazosin HCl (C247), dopamine HCl (H8502), doxazosin mesylate (D9815), histamine (H7125), (-)-isoproterenol HCl (I6504), (R)-(-)-niguldipine HCl (N162), phenylephrine hydrochloride (P6126), prazosin HCl (P7791), phentolamine HCl (P7547), phenoxybenzamine HCl (B019), (±)-propranolol HCl (P0884), serotonin HCl (H9523), tamsulosin HCl (T1330), terazosin HCl (T4680), were purchased from Sigma-Aldrich. Rauwolscine HCL from Tocris. [7-methoxy-^{3}H]-prazosin and myo-[2-^{3}H(N)]-inositol from Perkin-Elmer. SNAP-782 substrate (S9142S) from New England Biolabs. Epic 384 well glass-bottomed biosensor plates from Corning Inc.

Cell culture and transfections

Human SW480 colon carcinoma cells were grown in Dulbecco's modified Eagle's medium (DMEM) supplemented with 10% fetal bovine serum and 2 mM L-glutamine. For SNAP-α_{1B}-AR studies, cells were transfected with 1mg/ml polyethylenimine (PEI) and indicated concentrations of cDNA constructs, then assayed 48 hr post transfection.

Label-free dynamic mass redistribution assays

Label-free dynamic mass redistribution (DMR) assays were performed using a method derived from previously documented studies (Fang et al, 2006; Fang et al, 2007). SW480 cells (passage number 3-10) were seeded at ~500k/well in Corning Epic sensor microplates and cultured for 24 hr in DMEM + fetal bovine serum. On the day of the experiment, cells were washed 3x with HBSS buffer and transferred to the Corning Epic BT reader, which was permanently housed in a Thermo cell culture incubator @37°C with 5% CO_2, as this magnified the amplitude of recorded DMR responses. Cells were incubated with antagonists dissolved in HBSS for at least 1 hr prior

to adding agonist to ensure that equilibrium between antagonist and receptor had been reached, during which baseline DMR measurements were recorded. All compounds were added using a Sorenson Biosciences 96-well Benchtop Pipettor. Agonist DMR responses were recorded for 1 hr. Raw data were exported to Microsoft Excel using Epic Analyzer Software, and then imported into GraphPad Prism software to calculate agonist (potency, intrinsic activity) and antagonist (affinity) properties. Agonist concentration-response curves were fit using variable slope non-linear regression to determine potency (EC_{50}) and Hill slope. Y-axis values on raw DMR data and agonist DMR concentration-response curves represent the shift in light wavelength in picometers (pm) as a result of dynamic mass redistribution (DMR). Schild Plot analyses were performed when appropriate using a method derived from that first described in (Arunlakshana and Schild, 1959). Schild data were calculated for each experimental n (each having 4 replicates), and final Schild plots were calculated as the mean ± SEM of each experimental value. Schild plots were fit using linear regression analysis. Non-linear regression analysis was also used to determine if antagonist Schild slopes were significantly different than 1. Apparent affinity (pK_B) was calculated using the equation $pK_B = \log (DR-1) - \log [B]$. Control experiments were performed demonstrating antagonists used in this study did not stimulate significant DMR responses (see Supplemental Figure 1).

Quantitative reverse-transcriptase polymerase chain reaction (qRT-PCR) assays

Total RNA was isolated from SW480 cells using NucleoSpin RNA isolation kit according to manufacturer's instructions (Macherey-Nagel). One-step qRT-PCR reactions were carried out in a final volume of 20 μL that included: 2 μL of template RNA (25 ng final concentration), 0.8 μL forward and reverse primer (10 μM final concentration), 0.4 μL ROX reference dye, 10 μL of 2x one step SYBR RT-PCR Buffer, and 5.2 μL of RNase free H_2O using the One Step SYBR PrimeScript RT-PCR kit (Clontech). Primers used for qRT-PCR analysis were:

α_{1A} Forward: 5'-TGCCAGATCAACGAGGAGC-3', Reverse: 5'-GGCGTTTTTCCGATGGATGC-3';

JPET Fast Forward. Published on February 14, 2017 as DOI: 10.1124/jpet.116.237255
This article has not been copyedited and formatted. The final version may differ from this version.

α_{1B} Forward: 5'-CTTTCACGAGGACACCCTTAGC-3', Reverse: 5'-GCCCAACGTCTTAGCTGCTT-3';

α_{1D} Forward: 5'-CTCCAGCCTGTCGCACAAG-3', Reverse: 5'-TGTAGTCGGCCAATTCGTAGG-3';

β2 Forward: 5'-TGGTGTGGATTGTGTCAGGC-3', Reverse: 5'-GGCTTGGTTCGTGAAGAAGTC-3';

APRT Forward: 5'-GGCCGCATCGACTACATCG-3', Reverse: 5'-CTCAGCCTTCCCGTACTCC-3'.

qRT-PCR reactions were performed using the following protocol: 42°C for 5 min; 95°C for 5 sec; 60°C for 20 sec. Melt curve data were collected from 60°C to 95°C at a ramping rate of 0.2°C per second. qRT-PCR reactions were performed in quadruplicate on a Stratagene Mx3000 Real Time PCR system. Relative expression values of each genes of interest were normalized to the expression value of housekeeping gene adenine phosphoribosyltransferase (APRT).

Radioligand binding assays

Cell membranes were prepared from cultured SW480 cells via scraping and polytron grinding 3 times for 30 sec. Lysates were resuspended in ice cold phosphate buffered saline (PBS). Protein concentration was determined with an Eppendorf D30 BioPhotometer. 100 μL of PBS containing 100 ug of resuspended cell lysates were incubated with 100 μL of varying concentrations of [^{3}H]-prazosin for 30 min at 37C with gentle shaking, in the absence (representing Total [^{3}H]-prazosin bound) or presence of 100 μM of the non-selective α-AR antagonist phentolamine (representing Non-specific [^{3}H]-prazosin bound). Samples were then subjected to Brandel vacuum filtration (Brandel, Gaithersburg, MD). Filters were incubated with 5 mL liquid scintillation fluid and counted with a Tri-Carb 2200 CA liquid scintillation analyzer (Packard Instrument Co. Inc., Rockville, MD). Data were converted from CPM to fmol/mg protein (http://www.graphpad.com/quickcalcs/radcalcform/), and specific bound was calculated as Total Bound – Non-Specific Bound. Specific bound data were fit with one-site specific binding saturation analysis using GraphPad Prism 6 software. Data are expressed as mean ± SEM.

JPET Fast Forward. Published on February 14, 2017 as DOI: 10.1124/jpet.116.237255
This article has not been copyedited and formatted. The final version may differ from this version.

Phosphoinositol hydrolysis assays

SW480 cells were pre-labeled with 1 mCi/mL [^{3}H]-myo-inositol. After 48 hrs, cells were stimulated with 100 μM phenylephrine for 1 h in HBSS buffer + 10 mM LiCl. Total inositol phosphates were purified via Dowex ion exchange chromatography using the method described in (Lyssand et al, 2008). Data were analyzed with GraphPad Prism 6 software and expressed as mean ± SEM.

SNAP protein gels

SW480 cells were transfected with empty SNAP vector or SNAP-tagged α_{1B}-AR cDNA using the previously described PEI transfection method. 48 hours after transfection, cells were lysed with 50 mM Tris-HCl, 150 mM NaCl, 1% NP40, and 0.1% Tween 20 buffer. 0.5 μM BG-782 substrate and 1 mM DTT were added to lysates and samples were incubated for 30 minutes @37°C in the dark. Approximately 10 ug of cell lysates were run on 8-10% gels using SDS-PAGE. Gels were imaged using the LI-COR Odyssey Scanner. Protein band size was determined by comparison with PageRuler Prestained NIR Protein Ladder (Thermo #26635).

Cell proliferation and viability

Cells grown in DMEM supplemented with 10% FBS were harvested using trypsin and seeded in DMEM supplemented with 1% FBS in 96 well plates (5000 cells per well). 24 hours later, cells were treated by adding drugs to the cell culture media as previously described (Cherry et al, 2016). 3 days later, cell proliferation was measured using 5-Bromo-2'-deoxy-uridine (BrdU) cell proliferation ELISA (colorimetric) kit (Roche, Indianapolis, IN, USA) and cell viability using WST-1 (1:20, Roche, Pleasanton, CA) following manufacturer's protocols.

Results

One study has examined adrenergic receptor (AR) expression and function in SW480 cells (Masur et al, 2001). Specifically, using flow cytometry and primary antibodies targeting AR subtypes, this study suggested that SW480 cells express α_2 and β-ARs, and little to no α_1-ARs. To confirm this finding, we subjected SW480 cells to label-free dynamic mass redistribution assays, which measures agonist-stimulated changes in cell shape as a functional output. This highly quantitative technology detects deflections in the wavelength of polarized light reflected through glass-bottom microsensor plates (Camp et al, 2016). Up to 1 picometer changes in wavelength are reliably detected, thereby permitting detection of minute changes in cell shape stimulated by endogenous ARs. Our first set of experiments examined SW480 DMR responses stimulated by AR subtype selective agonists in real-time for 60 min. Raw DMR tracings are displayed in Figures 1A-E, which were then used to construct agonist-concentration curves at t = 60 min (Fig. 1F) to calculate agonist potencies and intrinsic activities (Table 1). As shown in Fig. 1A, the endogenous catecholamine norepinephrine (NE) stimulated robust, positive DMR responses in a concentration-dependent manner, presumably through the activation of β- and α_2-ARs previously demonstrated to be expressed by this cell type (Masur et al, 2001). Accordingly, the β-AR selective agonist isoproterenol (Fig. 1B) and the α_2-AR partial agonist clonidine (Fig. 1C) stimulated weaker DMR responses than those observed with NE. Clonidine was the most potent adrenergic agonist (Table 1). 5-HT (Fig. 1E) and histamine (data not shown) produced no significant DMR responses, suggesting members of these essential GPCR receptor families are not endogenously expressed by SW480 cells.

Unexpectedly, the α_1-AR selective agonist phenylephrine stimulated positive DMR responses with higher intrinsic activity (IA = 0.68) than both clonidine and isoproterenol, suggesting that functional α_1-ARs are present in SW480 cells, in direct contrast to the findings of previous studies (Masur et al, 2001).

Because DMR assays are thought to measure the summation of all cell signaling events, the possibility exists that the observed phenylephrine effects are a result of non-α_1-AR signaling mechanisms. Phenylephrine has been reported to activate β-ARs in human vascular beds (Torp et al, 1985), rabbit left ventricle (Wagner et al, 1974) and guinea-pig ventricles (Chess-Williams et al, 1990), depending on the relative density of α- versus β-ARs expressed. Thus, we assayed the efficacy of AR subtype-selective antagonists to block phenylephrine-stimulated DMR responses. If the observed phenylephrine DMR events are occurring via direct α_1-AR stimulation, we expect α_1-AR antagonists to inhibit phenylephrine responses at concentrations in the range of their reported nanomolar affinities. Saturating concentrations of the β-AR antagonist propranolol produced no significant changes in the phenylephrine DMR concentration response curve (Fig. 2A), nor did the α_2-AR antagonist rauwolscine (Fig. 2B), suggesting that phenylephrine DMR responses are not a result of β or α_2-AR receptor activation. By sharp contrast, pre-treating cells for 1 h with 100 nM of the α_1/α_2-AR irreversible antagonist phenoxybenzamine abolished phenylephrine DMR responses (Fig. 2C). Likewise, the competitive α_1/α_2-AR antagonist phentolamine produced progressive rightward shifts in phenylephrine concentration-response curve with successive half-log molar increments (Fig. 2D). Phenylephrine potencies in the absence and presence of phentolamine were determined and used to calculate phentolamine affinity using Schild regression analysis (Arunlakshana and Schild, 1959). Phentolamine inhibited phenylephrine DMR responses with pA_2 = -6.93, or 117 nM (Fig. 2E, Table 2), which is within the range of previously reported values for binding the α_{1B}-AR subtype (Morrow et al, 1986; Hong et al, 2005; Bavadekar et al, 2008).

We next assayed the affinity of the quinazoline α_1-AR selective antagonists doxazosin (Fig. 3A,B), terazosin (Fig. 3C,D) and prazosin (Fig. 3E,F) for inhibiting phenylephrine DMR responses. All three antagonists produced progressive rightward shifts in DMR concentration-response curves facilitating Schild regression analysis to calculate antagonist pA_2 values (listed in

Table 2). The affinities for terazosin and doxazosin are consistent with previously reported affinity values for antagonizing α_1-AR stimulated contractions of the rabbit (Martin et al, 1997) and human prostate (Muramatsu et al, 1998; Kenny et al, 1996). However, the observed prazosin DMR affinity is appreciably lower than what is reported in isolated tissue *in vitro* contraction assays examining the three α_1-AR subtypes (Docherty, 2010). Rather, our observed prazosin affinity value is within the range of the elusive "α_{1L}-adrenoceptor", or low-affinity α_1-AR prazosin binding site previously documented to be present in dog saphenous vein (Muramatsu et al, 1990), rat small mesenteric artery (Stam et al, 1999), rabbit urinary tract (Van der Graaf et al, 1997), rat portal vein (Digges et al, 1983) and rat vas deferens (Muramatsu et al, 1996). Thus, the lack of effect of β and α_2-AR antagonists, and the pronounced inhibition of phenylephrine DMR responses by mixed α_1/α_2-AR and α_1-AR selective antagonists indicates SW480 cells express functional α_1-ARs.

We next sought to identify the specific α_1-AR subtype(s) expressed by comparing the ability of various α_1-AR subtype selective antagonists to inhibit phenylephrine DMR responses. The antagonists tested included tamsulosin ($\alpha_{1A/D}$-AR selective), 5-methylurapidil and niguldipine (α_{1A}-AR selective), cyclazosin (α_{1B}-AR selective) and BMY7378 (α_{1D}-AR selective). All antagonist functional data are compiled in Table 2.

BMY7378 inhibited DMR responses with pA_2 = -6.87, or 134 nM (Fig. 4A,B), which is significantly lower than previously reported BMY 7378 functional affinities for inhibiting α_{1D}-AR mediated contraction of rat (Goetz et al, 1995; Kenny et al, 1995; Indra et al, 2002; Cleary et al, 2005) or mouse thoracic aorta (Yamamoto et al, 2001), and more indicative of an α_{1A} or α_{1B} affinity for this antagonist. Accordingly, the $\alpha_{1A/D}$-AR antagonist tamsulosin blocked phenylephrine stimulated DMR (Fig. 4C) with significantly lower apparent affinity (1 μM tamsulosin $pK_B = -6.83 \pm 0.08$) than previously reported tamsulosin pA_2 values for blocking the α_{1A} or α_{1D}-AR subtypes (Noble et al, 1997). The lack of α_{1A}-AR contribution to phenylephrine

responses was supported by the limited ability of α_{1A}-AR antagonists 5-methylurapidil (Fig. 4D) and niguldipine (Fig. 4E) to antagonize phenylephrine stimulated DMR responses. Interestingly, maximum phenylephrine DMR values were significantly decreased with increasing concentrations of tamsulosin, 5-methylurapidil and niguldpine. This observation demonstrates a potential limitation of using label-free DMR assays to calculate antagonist pA_2 values. Label-free DMR assays are thought to measure the summation of all downstream signaling events following GPCR activation (Fang et al, 2006; Fang et al, 2007; Schroder et al, 2010). Thus, if an α_1-AR antagonist binds and alters the activity of off-target proteins essential to the α_1-AR signaling cascade, this may result in an alteration in the magnitude of the DMR output. For example, niguldipine, a member of the dihydropyridine family of anti-hypertensives, inhibits both L-type Ca^{2+} channels (Boer et al, 1989) and bTREK-1 K^+ channels (Liu et al, 2007), such that decreases in maximum phenylephrine DMR responses observed at μM concentrations of niguldipine may be a result of disrupted electrochemical gradients. As such, the observed antagonist-dependent decreases in phenylephrine maximal DMR responses precludes pA_2 determination for tamsulosin, 5-methylurapidil or niguldipine. Regardless, the inability of BMY7378, tamsulosin, 5-methylurapidil or niguldipine to antagonize phenylephrine-stimulated DMR responses in SW480 with high affinity strongly suggests the α_{1A} and α_{1D} subtypes do not functionally contribute to phenylephrine responses. Conversely, the α_{1B}-AR selective antagonist cyclazosin potently inhibited phenylephrine responses with pA_2 = -8.37, or 4.26 nM (Fig. 4F, G), consistent with reported affinities for blocking α_{1B}-AR mediated contraction of rabbit thoracic aorta (Marucci et al, 2005). Given the α_{1B}-AR antagonist cyclazosin produced the most potent inhibition of phenylephrine DMR responses in SW480 cells, we hypothesize SW480 cells express predominantly the α_{1B}-AR subtype.

Label-free DMR pharmacological results were subsequently validated with quantitative reverse-transcriptase polymerase chain reaction (qPCR) assays. Internal primers directed against

individual α_1-AR subtypes and the β2-AR were used to measure relative mRNA concentrations expressed as cycle threshold (CT) fold. All values were compared to adenine phosphoribosyltransferase (APRT) levels as a reference house-keeping gene. As shown in Figure 5A, α_{1B}-AR mRNA levels were 2.53 ± 0.09 fold greater than APRT, whereas α_{1A}-AR (0.02 ± 0.06) and α_{1D}-AR (6 x 10^{-4} ± 0.28) mRNA levels were barely detectable. β2-AR mRNA levels (0.09 ± 0.04) were greater than α_{1A}- and α_{1D}-AR, yet significantly lower than α_{1B}-AR.

Thus, SW480 cells produce relatively high levels of α_{1B}-AR mRNA and robust phenylephrine-stimulated label-free DMR responses inhibited by the α_{1B}-AR selective antagonist cyclazosin. Yet, α_1-ARs are reported as minimally detectable in previous flow cytometry assays (Masur et al, 2001). To clarify this discrepancy, we quantified endogenous α_{1B}-AR functional receptor density with [^{3}H]-prazosin radioligand binding and phosphoinositol hydrolysis assays. As a positive control we included SW480 cells transfected with N-terminal SNAP-epitope tagged α_{1B}-ARs. SNAP protein gels demonstrated 3 ug of SNAP-α_{1B}-AR cDNA was optimal for ensuring SW480 cell viability and maximal SNAP-α_{1B}-AR protein levels (Fig. 5B, denoted with arrow at ~ 76.6 kDa). Remarkably, we did not detect significant levels of endogenous α_{1B}-AR binding sites (<10 fmol/mg protein) in SW480 cell lysates with [^{3}H]-prazosin saturation radioligand binding assays, whereas transfecting SNAP-α_{1B}-AR induced a robust increase in receptor density (Bmax to 59.3 ± 10.7 fmol/mg protein, Fig. 5C). Phosphoinositol hydrolysis assays produced equivalent results (Fig. 5D). Specifically, application of 100 μM phenylephrine did not generate significant increases in WT SW480 cellular inositol phosphate levels, yet produced a 62.1% increase in inositol phosphate formation in SW480 cells transfected with SNAP-α_{1B}-AR. Congruent with this finding, maximal phenylephrine-stimulated DMR responses were enhanced by 25.8% in SW480 cells when transfected with SNAP-α_{1B}-AR (Fig. 5E). Taken together, these data demonstrate that SW480 cells express low levels of functional α_{1B}-ARs that

are undetectable with radioligand binding and reductionist functional assays, but are robustly detectable with label-free DMR assays.

While it is has been shown that AR stimulation induces migration of cultured SW480 cells (Masur et al, 2001), this study used norepinephrine as the adrenergic agonist and thus the AR subtype(s) involved remain unclear. With the discovery that SW480 cells express low level of functional α_{1B}-ARs, we sought to delineate the effect of β and α_1-ARs stimulation on SW480 cell viability and proliferation. β-AR stimulation with isoproterenol produced a dose-dependent decrease in both cell viability and proliferation (Figure 6A). Note that the anti-proliferative effects of isoproterenol were marginally greater than its anti-viability effects. Conversely, α_1-AR stimulation with phenylephrine produced a striking increase in cell viability, with no significant effects on cell proliferation (Figure 6B). The pro-survival effects of phenylephrine were antagonized by the α_1-AR antagonists terazosin, cyclazosin, phenoxybenzamine and phentolamine (Figure 6C). These results show that SW480 cells express low densities of functional α_{1B}-ARs, that when activated, are pro-survival.

Discussion

With the ongoing and increasing usage of small molecules targeting adrenergic signaling mechanisms for the treatment of cardiovascular disease, central nervous system disorders and numerous other indications, understanding whether these medicines also influence tumor growth and/or metastasis is of critical importance. Accordingly, identifying subtypes of adrenergic receptors (ARs) expressed by specific cancer cells, characterizing the action of small molecules targeting this receptor family, and their resulting effect on tumor cell fate will provide critical information that might drive patient-specific pharmacotherapy. In this study we illustrate the inherent power of label-free dynamic mass redistribution signaling technology to identify low density, yet highly-functional ARs in SW480 carcinoma cancer cells. Moreover, to the best of our

knowledge, our study represents the first to combine label-free DMR assays with Schild regression analysis of antagonist affinities to facilitate pharmacological characterization of cancer cell specific expression of endogenous GPCR subtypes. Based on these results, we provide evidence that antagonists targeting both α_{1B}-AR and β-AR may significantly effect cancer cell fate.

The effects of chronic AR stimulation on human health and disease have been extensively studied and documented. Thus far, the overwhelming majority of the data indicates chronic β-AR stimulation produces negative outcomes on cancer prognosis. Epidemiological data compiled from breast cancer outcomes of patients on chronic β-blocker therapy had a 57% reduced risk of metastasis and 71% reduction in mortality after 10 years (Powe et al, 2010). A subsequent study discovered brain metastasis derived from breast cancer cells have increased β2-AR mRNA and protein expression levels, and exhibit enhanced cell proliferation and migration (Choy et al, 2016). Chronic β-AR activation induced by stress promotes colon cancer metastasis (Zhao et al, 2015), possibly through trans-activation of the EGFR-Akt/ERK pathway (Chin et al, 2016). Accordingly, β-AR blockade has been shown to be an effective treatment in experimental models of colon cancer (Barbieri et al, 2015; Sorski et al, 2016) and reduces the incidence of colon cancer in human populations (Chang et al, 2015). Contrary to these findings, we found β-AR activation decreased SW480 cell viability and proliferation, similar to what has been reported in cardiomyocytes during heart failure, where prolonged β-AR stimulation leads cell death, fibrosis and adverse remodeling (reviewed in Lefkowitz et al, 2000).

Significantly less information exists on the role of α_1-AR activation in cancer outcomes. Studies investigating the effects of chronic α_1-AR stimulation on cell survival from cardiovascular studies provide valuable insights (Furberg et al, 2002). A major revelation of the groundbreaking Anti-Hypertensive and Lipid-Lowering treatment to prevent Heart Attack Trial (ALLHAT) was the increased incidence of deleterious cardiovascular events in the doxazosin-

treatment arm, forcing an early termination of this portion of the study (Piller et al, 2002). This single observation has significantly diminished the use of α_1-AR antagonists for hypertension, heart failure and other cardiovascular diseases. Subsequent basic science studies showed that α_1-AR stimulation inhibits apoptosis in *in vitro* and *in vivo* and enhances ischemic preconditioning in human volunteers via activating pro-survival mechanisms such as induction of fetal gene transcription, increased protein synthesis, enhanced glycolysis, activation of ERK, protein kinase C, and others (reviewed in Jensen et al, 2011). Additionally, a series of elegant KO mice studies show that knocking the α_{1A} and α_{1B}-AR subtypes induces maladaptive cardiac morphological alterations, resulting in diminished cardiac output, impaired exercise tolerance and enhanced mortality induced by transverse aortic constriction (TAC), suggesting α_1-ARs are pro-survival in cardiomyocytes (O'Connell et al, 2006). Despite these significant studies, the specific contributions of individual α_1-AR subtypes to the pro-survival phenotype in various cancers remains unclear.

We found that α_{1B}-AR stimulation enhanced SW480 cell survival, despite their relatively low expression. Interestingly, mice overexpressing constitutively active α_{1B}-AR mutants display a host of maladaptive phenotypes including cardiac hypertrophy post TAC (Wang et al, 2000), depression-like behavior (Doze et al, 2009), age-related apoptotic neurodegeneration (Zuscik et al, 2000; Papay et al, 2000), and reduced life-span (Collette et al, 2014). Taken together, the effects of α_{1B}-AR stimulation on cell outcome may be directly correlated to their functional expression levels, with low to moderate expression of α_{1B}-ARs be pro-survival, whereas overexpression promotes morphological changes leading to cell death. Further studies are needed to clarify the effect of chronic α_{1B}-AR stimulation on cancer cell fate, and if these effects are specific to colon carcinoma cells.

In summary, we leveraged the power of label-free DMR signaling technology to identify and characterize low-density α_{1B}-ARs previously undetectable with traditional experimental

approaches used to quantify GPCR functional expression levels in cell culture (i.e. as measured by flow cytometry, radioligand binding or reductionist functional assays), which when activated, increase the survival of human SW480 colon carcinoma cells. To our knowledge, this study is the first to examine the effects of α_{1B}-AR stimulation on human colon carcinoma cell fate. Thus, label-free DMR should prove useful for characterizing membrane signaling proteins functionally expressed on specific carcinoma cell types, thereby facilitating their investigation as potential anti-neoplastic targets using available therapeutic agents, or to predict the side effects of concurrently-used medications on tumor cell outcome. As health-care systems move towards the era of precision medicine, the translational advantages of label-free technology provides a unique opportunity to drive patient-specific pharmacotherapy. Our discovery that α_{1B}-ARs are pro-survival in SW480 colon carcinoma cells may have relevance for the increasing number of patients taking α_1-AR antagonists for benign prostatic hypertrophy, post-traumatic stress disorder and/or cardiovascular disease. Thus, further investigation into the effects of α_1-AR stimulation on colon carcinoma cell fate are warranted.

Author Contributions

Participated in research design: Harris, Lee, Stella, and Hague.

Conducted experiments: Harris, Park, Lee, Xu, and Hague.

Contributed new reagents or analytic tools: None.

Performed data analysis: Harris, Lee, Stella, and Hague.

Wrote or contributed to the writing of the manuscript: Harris, Stella, and Hague.

References

Anglin IE, Glassman DT, and Kyprianou N (2002) Induction of prostate apoptosis by α_1-adrenoceptor antagonists: mechanistic significance of the quinazoline component. *Prostate Cancer and Prostatic Diseases* 5(2): 88-95.

Arunlakshana O and Schild HO (1959) Some quantitative uses of drug antagonists. *Br J Pharmacol Chemother* 14(1):48-58.

Barbieri A, Bimonte S, Palma G, Luciano A, Rea D, Guidice A, Scognamiglio G, La Mantia E, Franco R, Perdona S, De Cobelli O, Ferro M, Zappavigna S, Stiuso P, Caraglia M, and Arra C (2015) The stress hormone norepinephrine increases migration of prostate cancer cells *in vitro* and *in vivo*. *Int J Oncol* 47(2): 527-34.

Bavadekar SA, Hong S-S, Lee S-I, Miller DD, and Feller DR (2008) Bioisosteric phentolamine analogs as selective human α_2- versus α_1-adrenoceptor ligands. *Eur J Pharmacol* 590(1-3): 53-60.

Boer R, Grassegger A, Schudt C, and Glossmann H (1989) (+)-Niguldipine binds with very high affinity to Ca^{2+} channels and to a subtype of α_1-adrenoceptors. *Eur J Pharmacol* 172(2): 131-45.

Camp ND, Lee K-S, Wacker-Mhyre JL, Kountz TS, Park JM, Harris DA, Estrada M, Stewart A, Wolf-Yadlin A, and Hague C (2015) Individual protomers of a G protein-coupled receptor dimer integrate distinct functional modules. *Cell Discovery*. 1, doi:10.1038/celldisc.2015.11

Camp ND, Lee KS, Cherry A, Wacker-Mhyre JL, Kountz TS, Park JM, Harris DA, Estrada M, Stewart A, Stella N, Wolf-Yadlin A, and Hague C (2016) Dynamic mass redistribution reveals

diverging importance of PDZ-ligands for G protein-coupled receptor pharmacodynamics. *Pharmacol Res* 105:13-21.

Catapano LA and Manji HK (2007) G protein-coupled receptors in major psychiatric disorders. *Biochim Biophys Acta* 1768(4): 976-993.

Chang PY, Huang WY, Lin CL, Huang TC, Wu YY, Chen JH, and Kao CH (2015) Propranolol reduces cancer risk: a population-based cohort study. *Medicine (Baltimore)* 94(27):e1097.

Cherry AE, Haas BR, Naydenov AV, Fung S, Xu C, Swinney K, Wagenbach M, Freeling J, Canton DA, Coy J, Horne EA, Rickman B, Vicente JJ, Scott JD, Ho RJ, Liggitt D, Wordeman L, and Stella N (2016) ST-11: a new brain-penetrant microtubule-destabilizing agent with therapeutic potential for glioblastoma multiforme. *Mol Cancer Ther* 15(9): 2018-29.

Chess-Williams RG, Williamson KL, and Broadley KJ (1990) Whether phenylephrine exerts inotropic effects through α- or β-adrenoceptors depends upon the relative receptor populations. *Fundam Clin Pharmacol* 4(1): 25-37.

Chin CC, Li JM, Lee KF, Huang YC, Wang KC, Lai HC, Cheng CC, Kuo YH, and Shi CS (2016) Selective β2-AR blockage suppresses colorectal cancer growth through regulation of EGFR-Akt/ERK1/2 signaling, G1-phase arrest, and apoptosis. *J Cell Physiol* 231(2): 459-72.

Choy C, Raytis JL, Smith DD, Duenas M, Neman J, Jandial R, and Lew MW (2016) Inhibition of β2-adrenergic receptor reduces triple-negative breast cancer metastases: the potential benefit of perioperative β-blockade. *Oncol Rep* 35(6): 3135-42.

Cleary L, Murad K, Bexis S, and Docherty JR (2005) The α_{1D}-adrenoceptor antagonist BMY 7378 is also an α_{2C}-adrenoceptor antagonist. *Auton Autacoid Pharmacol* 25(4): 135-41.

Cole SW, and Sood AK (2011) Molecular Pathways: β-adrenergic signaling in cancer. *Clin Cancer Res* 18(5): 1201-6.

Collette KM, Zhou XD, Amoth HM, Lyons MJ, Papay RS, Sens DA, Perez DM, and Doze VA (2014) Long-term α_{1B}-adrenergic receptor activation shortens lifespan, while α_{1A}-adrenergic receptor stimulation prolongs lifespan in association with decreased cancer incidence. *Age* 36(4): 9675.

Digges KG, and Summers RJ (1983) Characterization of postsynaptic α-adrenoceptors in rat aortic strips and portal veins. *Br J Pharmacol* 79(3): 655-65.

Docherty JR (2010) Subtypes of functional α_1-adrenoceptor. *Cell Mol Life Sci* 67(3): 405-17.

Doze VA, Handel EM, Jensen KA, Darsie B, Luger EJ, Haselton JR, Talbot JN, and Rorabaugh BR (2009) α_{1A} and α_{1B}-adrenergic receptors differentially modulate antidepressant-like behavior in the mouse. *Brain Res* 1285: 148-57.

Fang Y, Ferrie AM, Fontaine NH, Mauro J, and Balakrishnan J (2006) Resonant waveguide grating biosensor for living cell sensing. *Biophys J* 91: 1925-1940.

Fang Y, Li G, and Ferrie AM (2007) Non-invasive optical biosensor for assaying endogenous G protein-coupled receptors in adherent cells. *J Pharmacol Toxicol Methods* 55: 314-322.

Furberg CD, et al. (2002) Major outcomes in high-risk hypertensive patients randomized to angiotensin-converting enzyme inhibitor or calcium channel blocker vs diuretic: The Antihypertensive and Lipid-Lowering treatment to prevent heart attack trial (ALLHAT). *JAMA* 288(23): 2981-2997.

Goetz AS, King HK, Ward SD, True TA, Rimele TJ, and Saussy DL (1995) BMY 7378 is a selective antagonist of the D subtype of α_1-adrenoceptors. *Eur J Pharmacol* 272(2-3):R5-6.

Hong S-S, Bavadekar SA, Lee S-I, Patil PN, Lalchandani SG, Feller DR, and Miller DD (2005) Biosteric phentolamine analogs as potent α-adrenergic antagonists. *Bioorg Med Chem Lett* 15: 657-64.

Indra B, Matsunaga K, Hoshino O, Suzuki M, Ogasawara H, Muramatsu I, Taniguchi T, and Ohizumi Y (2002) (±)-Domesticine, a novel and selective α_{1D}-adrenoceptor antagonist in animal tissue and human α_1-adrenoceptors. *Eur J Pharmacol* 445(1-2): 21-29.

Jensen BC, O'Connell TD, and Simpson PC (2011) α_1-adrenergic receptors: targets for agonist drugs to treat heart failure. *J Mol Cell Cardiol* 51(4): 518-28.

Kenny BA, Chalmers DH, Philpott PC, and Naylor AM (1995) Characterization of an α_{1D}-adrenoceptor mediating the contractile response of rat aorta to noradrenaline. *Br J Pharmacol* 115(6): 981-6.

Kenny BA, Miller AM, Williamson IJ, O'Connell J, Chalmers DH, and Naylor AM (1996) Evaluation of the pharmacological selectivity profile of α_1-adrenoceptor antagonists at prostatic α_1-adrenoceptors: binding, functional and *in vivo* studies. *Br J Pharmacol* 118(4): 871-88.

Kyprianou N, Vaughan TB, and Michel MC (2009) Apoptosis induction by doxazosin and other quinazoline α_1-adrenoceptor antagonists: a new mechanism for cancer treatment? *Naunyn Schmiedebergs Arch Pharmacol.* 380(6): 473-7.

Kountz TS, Lee KS, Aggarwal-Howarth S, Curran E, Park JM, Harris DA, Stewart A, Hendrickson J, Camp ND, Wolf-Yadlin A, Wang EH, Scott JD, and Hague C (2016) Endogenous N-terminal domain cleavage modulates α_{1D}-adrenergic receptor pharmacodynamics. *J Biol Chem* 291(35): 18210-21.

Lefkowitz RJ, Rockman HA, and Kock WJ (2000) Catecholamines, cardiac β-adrenergic receptors, and heart failure. *Circulation* 101: 1634-37.

Liu H, Enyeart JA, and Enyeart JJ (2007) Potent inhibition of native TREK-1 K^+ channels by selected dihydropyridine Ca^{2+} channel antagonists. *J Pharmacol Exp Ther* 323(1): 39-48.

Lyssand JS, DeFino MC, Tang XB, Hertz AL, Feller DB, Wacker JL, Adams ME, and Hague C. (2008) Blood pressure is regulated by an α_{1D}-adrenergic receptor/dystrophin signalosome. *J Biol Chem* 283(27): 18792-800.

Lyssand JS, Whiting JL, Lee KS, Kastl R, Wacker JL, Bruchas MR, Miyatake M, Langeberg LK, Chavkin C, Scott JD, Gardner RG, Adams ME, and Hague C (2010) α-dystrobrevin-1 recruits α-catulin to the α_{1D}-AR/DAPC signalosome. *Proc Natl Acad Sci U.S.A.* 107: 21854-21859.

Martin DJ, Lluel P, Guillot E, Coste A, Jammes D, and Angel I (1997) Comparative α_1-adrenoceptor subtype selectivity and functional uroselectivity of α_1-adrenoceptor antagonists. *J Pharmacol Exp Ther* 282(1): 228-235.

Marucci G, Angeli P, Buccioni M, Gulini U, Melchiorre C, Sagratini G, Testa R, and Giardina D (2005) (+)-cyclazosin, a selective α_{1B}-adrenoceptor antagonist: functional evaluation in rat and rabbit tissues. *Eur J Pharmacol* 522(1-3): 100-7.

Masur K, Niggemann B, Zanker KS, and Entschladen F (2001) Norepinephrine-induced migration of SW 480 colon carcinoma cells is inhibited by β-blockers. *Cancer Res* 61(7): 2866-69.

Morrow AL and Creese I (1986) Characterization of α_1-adrenergic receptor subtypes in rat brain: a reevaluation of [^{3}H]WB4104 and [^{3}H]Prazosin binding. *Mol Pharmacol* 29:321-330.

Muramatsu I, Ohmura T, Kigoshi S, Hashimoto S, and Oshita M (1990) Pharmacological subclassification of α_1-adrenoceptors in vascular smooth muscle. *Br J Pharmacol* 99(1):197-201.

Muramatsu I, Takita M, Suzuki F, Miyamoto S, Sakamoto S, and Ohmura T (1996) Subtype selectivity of a new α_1-adrenoceptor antagonist, JTH-601: comparison with prazosin. *Eur J Pharmacol* 300(1-2): 155-7.

Muramatsu I, Taniguchi T, and Okada K (1998) Tamsulosin: α_1-adrenoceptor subtype-selectivity and comparison with terazosin. *Jpn J Pharmacol* 78:331-335.

Noble AJ, Chess-Williams R, Couldwell C, Furukawa K, Uchyiuma T, Korstanje C, and Chapple CR (1997) The effects of tamsulosin, a high affinity antagonist at functional α_{1A} and α_{1D}-adrenoceptor subtypes. *Br J Pharmacol* 120(2): 231-8.

O'Connell TD, Swigart PM, Rodrigo MC, Ishizaka S, Joho S, Turnbull L, Tecott LH, Baker AJ, Foster E, Grossman W, and Simpson PC (2006) α_1-adrenergic receptors prevent a maladaptive cardiac response to pressure overload. *J Clin Invest* 116(4): 1005-1015.

Papay R, Zuscik MJ, Ross SA, Yun J, McCune DF, Gonzalez-Cabrera P, Gaivin R, Drazba J, and Perez DM (2002) Mice expressing the α_{1B}-adrenergic receptor induces a synucleinopathy with excessive tyrosine nitration but decreased phosphorylation. *J Neurochem* 83(3): 623-34.

Partin JV, Anglin IE, and Kyprianou N (2003) Quinazoline-based α_1-adrenoceptor antagonists induce prostate cancer cell apoptosis via TGF-β signaling and IκBα induction. *Br J Cancer* 88(10): 1615-21.

Patel ND, and Parsons JK (2014) Epidemiology and etiology of benign prostatic hyperplasia and bladder outlet obstruction. *Indian J Urol* 30(2): 170-76.

Perez-Sayans M, Somoza-Martin JM, Barros-Angueira FB, Diz PG, Gandara Rey JM, and Garcia-Garcia A (2010) β-adrenergic receptors in cancer: therapeutic implications. *Oncol Res* 19(1): 45-54.

Piller LB, Davis BR, Cutler WC, Cushman JT, Wright JT Jr, Williamson JD, Leenen FH, Einhorn PT, Randall OS, Golden JS, Haywood LJ, and the ALLHAT Collaborative Research Group (2002) Validation of heart failure events in the antihypertensive and lipid lowering

treatment to prevent heart attack trial (ALLHAT) participants assigned to doxazosin and chlorthalidone. *Curr Control Trials Cardiovasc Med* 3(1): 10.

Powe DG, Voss MJ, Zanker KS, Habashy HO, Green AR, Ellis IO, and Entschladen F (2010) β-blocker drug therapy reduces secondary cancer formation in breast cancer and improves cancer specific survival. *Oncotarget* 1(7): 628-38.

Schroder R, Janssen N, Schmidt J, Kebig A, Merten N, Hennen S, Muller A, Blattermann S, Mohr-Andra M, Zahn S, Wenzel J, Smith NJ, Gomeza J, Drewke C, Milligan G, and Kostenis E (2010) Deconvolution of complex G protein-coupled receptor signaling in live cells using dynamic mass redistribution measurements. *Nat Biotechnol* 28(9): 943-9.

Sorski L, Melamad R, Matzner P, Lavon H, Shaashua L, Rosenne E, and Ben-Eliyahu S (2016) Reducing liver metastasis of colon cancer in the context of extensive and minor surgeries through β-adrenoceptors blockade and COX inhibition. *Brain Behav Immun* 1591(16):30138-6.

Stam WB, Van der Graaf PH, and Saxena PR (1999) Analysis of α_{1L}-adrenoceptor pharmacology in rat small mesenteric artery. *Br J Pharmacol* 127(3): 661-70.

Torp KD, Tschakovsky ME, Halliwill JR, Minson CT, and Joyner MJ (1985) β-receptor agonist activity of phenylephrine in the human forearm. *J Appl Physiol* 90(5): 1855-9.

Van der Graaf PH, Deplanne V, Duquenne C, and Angel I (1997) Analysis of α_1-adrenoceptors in rabbit lower urinary tract and mesenteric artery. *Eur J Pharmacol* 327(1): 25-32.

Wagner J, Endoh M, and Reinhardt D (1974) Stimulation by phenylephrine of adrenergic α- and β-receptors in the isolated perfused rabbit heart. *Naunyn-Schmiedebergs Arch Pharmacol* 282(3): 307-310.

Wang BH, Du XJ, Autelitano DJ, Milano CA, and Woodcock EA (2000) Adverse effects of constitutively active α_{1B}-adrenergic receptors after pressure overload in mouse hearts. *Am J Physiol Heart Circ* 279(3): H1079-H1086.

Yamamoto Y and Koike K (2001) Characterization of α_1-adrenoceptor-mediated contraction in the mouse thoracic aorta. *Eur J Pharmacol* 424(2): 131-40.

Zhao L, Xu J, Liang F, Li A, Zhang Y, and Sun J (2015) Effect of chronic psychological stress on liver metastasis of colon cancer in mice. *PLoS One* 10(10):e0139978.

Zuscik MJ, Sands S, Ross SA, Waugh DJ, Gaivin RJ, Morilak D, and Perez DM (2000) Overexpression of the α_{1B}-adrenergic receptor causes apoptotic neurodegeneration: multiple systems atrophy. *Nat Med* 6(12): 1388-94.

Footnotes

This work was supported by the National Institutes of Health [GM100893, DA014486, 5T32GM00775].

Figure Legends

Fig. 1. Agonist-stimulated dynamic mass redistribution (DMR) responses in human SW480 colon carcinoma cells. Raw label-free DMR responses were measured for the non-selective adrenergic receptor (AR) agonist norepinephrine (*A*), the β-AR selective agonist isoproterenol (*B*), the α_2-AR selective agonist clonidine (*C*), the α_1-AR selective agonist phenylephrine (*D*) and 5-hydroxytryptamine/5-HT (*E*). *F*, Data were used to construct concentration-response curves to calculate agonist potencies and intrinsic activities for stimulating DMR responses at t = 60 min (listed in Table 1). Data are mean ± SEM from 3-4 independent experiments performed with 4 replicates.

Fig. 2. Phenylephrine-stimulated SW480 dynamic mass redistribution responses (DMR) are blocked by α-adrenergic receptor (AR) antagonists. Label-free DMR responses were measured for the α_1-AR selective agonist phenylephrine in the absence and presence of (*A*) the β-AR antagonist propranolol, (*B*) the α_2-AR antagonist rauwolscine, (*C*) the irreversible α_1/α_2-AR antagonist phenoxybenzamine (*D*), or the competitive α_1/α_2-AR antagonist phentolamine. For each condition, concentration-response curves were constructed using DMR values obtained at t = 60 min, and used to calculate agonist potency. (*E*) Schild regression analysis of phentolamine affinity from data in (*D*). Data are mean ± SEM from 3 independent experiments performed with 4 replicates.

Fig. 3. Phenylephrine-stimulated SW480 dynamic mass redistribution (DMR) responses are blocked with high affinity by α_1-adrenergic receptor (AR) antagonists. Label-free DMR responses were measured for the α_1-AR selective agonist phenylephrine in the absence and presence of the α_1-AR selective antagonists (*A*) doxazosin, (*C*) terazosin, and (*E*) prazosin. For each condition, concentration-response curves were constructed using DMR values obtained at t = 60 min, from which agonist potencies were calculated for subsequent Schild regression analysis of affinity for doxazosin (*B*), terazosin (*D*) and prazosin (*F*). Data are mean ± SEM from 3 independent experiments performed with 4 replicates.

JPET Fast Forward. Published on February 14, 2017 as DOI: 10.1124/jpet.116.237255
This article has not been copyedited and formatted. The final version may differ from this version.

Fig. 4. Phenylephrine-stimulated SW480 dynamic mass redistribution (DMR) responses are blocked with high affinity by the α_{1B}-adrenergic receptor (AR) selective antagonist cyclazosin. Label-free DMR responses were measured for the α_1-AR selective agonist phenylephrine in the absence and presence of the α_{1D}-AR subtype selective antagonist BMY7378 (*A*, Schild regression analysis in *B*); the $\alpha_{1A/D}$-AR subtype selective antagonist tamsulosin (*C*); the α_{1A}-AR subtype selective antagonists 5-methylurapidil (*D*), and niguldipine (*E*); and the α_{1B}-AR subtype selective antagonist cyclazosin (*F*, Schild regression analysis in *G*). For each condition, concentration-response curves were constructed using DMR values obtained at t = 60 min. When appropriate, agonist potencies were calculated for subsequent Schild regression analysis of affinity. Data are mean ± SEM from 3 independent experiments performed with 4 replicates.

Fig. 5. SW480 cells express high levels of α_{1B}-adrenergic receptor (AR) mRNA and low densities of functional α_{1B}-ARs. *A*, Quantitative reverse transcriptase PCR was performed on mRNA isolated from SW480 cell lysates using internal primers targeted to the α_{1A} (ADRA1A), α_{1B} (ADRA1B), α_{1D} (ADRA1D) and β2 (ADRB2)-AR subtypes. Data were normalized as cycle threshold (CT) fold change relative to APRT mRNA levels and are as expressed as mean ± SEM (n = 2 with 3 replicates). *B*, Polyacrylamide gel electrophoresis of wild type SW480 cell lysates (MOCK lane), or SW480 cell lysates following transfection with empty pSNAP vector (SNAP), and 2, 3 or 5 ug of N-terminal SNAP-epitope tagged α_{1B}-AR cDNA. SNAP-α_{1B}-AR protein bands are denoted with black arrow on right (76.6 kDa). *C*, Saturation [^{3}H]-prazosin radioligand binding assays were performed on SW480 cell lysates transfected with empty pSNAP vector (■) or 3 ug of SNAP-α_{1B}-AR cDNA (■). Non-specific binding was determined with 10 μM phentolamine. Data are the mean ± SEM of 3 experiments with 3 replicates. *D*, Phosphoinositol hydrolysis assays were performed on SW480 cells transfected with empty pSNAP vector or 3 μg of SNAP-α_{1B}-AR cDNA. Cells were pre-incubated with 1 μCi of [^{3}H]-myoinositol for 48 h and treated with HBSS buffer or 100 μM phenylephrine for 1 h. Data are expressed as the mean ± SEM of 3 experiments performed in triplicate. ** (student's *t*-test, $p < 0.05$). *E*, Label-free dynamic mass redistribution (DMR) responses were measured for the α_1-AR selective agonist phenylephrine in SW480 cells transfected with empty pSNAP vector (■) or 3 ug of SNAP-α_{1B}-AR cDNA (■). Data are the mean ± SEM of 2 experiments with 4 replicates.

JPET Fast Forward. Published on February 14, 2017 as DOI: 10.1124/jpet.116.237255
This article has not been copyedited and formatted. The final version may differ from this version.

Fig. 6. Stimulation of β-adrenergic receptors (AR) decreases cell proliferation and viability and stimulation of α_{1B}-AR increases cell viability of SW480 cells. Changes in SW480 cell proliferation and viability in response to drug treatment was measured using Brd-U and WST-1 assays, respectively. The β-AR selective agonist isoproterenol produces concentration-dependent decreases in both cell proliferation and viability whereas the α_1-AR selective agonist phenylephrine increases cell viability without affecting proliferation (*B*). *C*, Phenylephrine-stimulated increases in cell viability (100 μM) were antagonized by 10 min pre-treatment with cyclazosin (CYS, 100 nM) terazosin (TRZ, 1 μM), phenoxybenzamine (PBZ, 300 nM) or phentolamine (PHN, 10 μM). Data are the mean ± SEM of 3 experiments with 4 replicates. ** $p < 0.01$ compared with vehicle treated cells (control) (one-way ANOVA with Dunnett's post hoc test).

JPET Fast Forward. Published on February 14, 2017 as DOI: 10.1124/jpet.116.237255
This article has not been copyedited and formatted. The final version may differ from this version.

Table 1. Pharmacological properties of GPCR agonists in SW480 cells . Agonist stimulated dynamic mass redistribution (DMR) concentration-response curves were constructed for responses measured at endogenous receptors expressed in SW480 cells. Log molar agonist potencies (pEC_{50}) were calculated using the time at which peak DMR response was observed. Intrinsic activities (IA) were calculated by setting norepinephrine maximal DMR responses equal to 1 and then normalizing other observed agonist maximal DMR values to this value. All data were analyzed with GraphPad Prism using non-linear regression curve analysis and are expressed as mean ± SEM of 3-4 independent experiments performed with 4 replicates. Max = maximum response observed in pm. IA = intrinsic activity. ND = not determined.

Agonist	pEC_{50}	EC_{50} (μM)	Max (pm)	IA
Norepinephrine	-5.96 ± 0.04	1.08	354.74 ± 4.72	1
Isoproterenol	-4.27 ± 0.13	54.4	151.35 ± 7.66	0.43
Clonidine	-6.52 ± 0.12	0.3	144.47 ± 13.2	0.41
Phenylephrine	-5.40 ± 0.03	13.9	238.21 ± 4.52	0.67
5-HT	ND	ND	ND	ND

JPET Fast Forward. Published on February 14, 2017 as DOI: 10.1124/jpet.116.237255
This article has not been copyedited and formatted. The final version may differ from this version.

Table 2. Pharmacological values used for α_1-AR subtype selective antagonist Schild regression analyses. Phenylephrine stimulated concentration-response curves were calculated for stimulating dynamic mass redistribution (DMR) responses in SW480 cells. Log molar agonist potencies (pEC_{50}) were calculated using the time at which peak DMR response was observed in the absence and presence of various α-AR antagonists (concentration of antagonist used shown in brackets for each phenylephrine pEC_{50} value). Agonist potencies were subsequently used to calculate antagonist affinity and slope via Schild regression analysis. All data were analyzed with GraphPad Prism and are expressed as mean ± SEM of 2-4 independent experiments performed with 4 replicates. ** indicates calculated Schild slope is significantly different than unity as determined by non-linear regression analysis including extra sum-of-squares F test to hypothetical value of 1. ^^ indicates agonist concentration-response curve Hill slope is <1 as determined by non-linear regression curve four parameter variable slope analysis. ND = not determined.

	Phenylephrine pEC_{50} ± SEM					Schild analysis	
Antagonist	**Control**	**Dose 1**	**Dose 2**	**Dose 3**	**Dose 4**	**pA_2**	**Slope**
Phentolamine	-5.12 ± 0.03	-4.52 ± 0.03 (300 nM)	-4.19 ± 0.04 (1 μM)	-3.54 ± 0.06 (3 μM)	-3.11 ± 0.1 (10 μM)	-6.93 ± 0.51	1.03 ± 0.08
Doxazosin	-5.56 ± 0.05	-5.24 ± 0.05 (10 nM)	-5.23 ± 0.03 (30 nM)	-4.86 ± 0.04 (100 nM)	-4.07 ± 0.08 (300 nM)	-7.76 ± 0.27	1.18 ± 0.34
Terazosin	-5.28 ± 0.05	-4.98 ± 0.11 (100 nM)	-4.52 ± 0.08 (300 nM)	-4.06 ± 0.14 (1 μM)	-------	-7.81 ± 0.25	0.93 ± 0.29
Prazosin	-5.70 ± 0.06	-5.29 ± 0.05 (100 nM)	-4.69 ± 0.05 (300 nM)	-4.38 ± 0.07^^ (1 μM)	-------	-7.47 ± 0.32	1.07 ± 0.21
Tamsulosin	-5.43 ± 0.06	-4.87 ± 0.07 (300 nM)	-4.54 ± 0.07 (1 μM)	-4.38 ± 0.1 (3 μM)	-4.05 ± 0.1 (10 μM)	ND	ND
5-Methylurapidil	-5.45 ± 0.1	-5.17 ± 0.14 (300 nM)	-4.84 ± 0.14 (1 μM)	-4.89 ± 0.25 (3 μM)	-4.21 ± 0.23 (10 μM)	ND	ND
Niguldipine	-5.65 ± 0.08	-5.08 ± 0.11 (3 μM)	-3.82 ± 0.15 (10 μM)	-------	-------	ND	ND
Cyclazosin	-5.42 ± 0.11	-4.86 ± 0.12 (10 nM)	-4.62 ± 0.09 (30 nM)	-4.01 ± 0.11 (100 nM)	-------	-8.37 ± 0.19	0.97 ± 0.21
BMY7378	-5.14 ± 0.03	-4.57 ± 0.05 (300 nM)	-4.13 ± 0.03 (1 μM)	-3.57 ± 0.07 (3 μM)	-3.21 ± 0.1 (10 μM)	-6.87 ± 0.47	1.06 ± 0.01

Fig. 1.

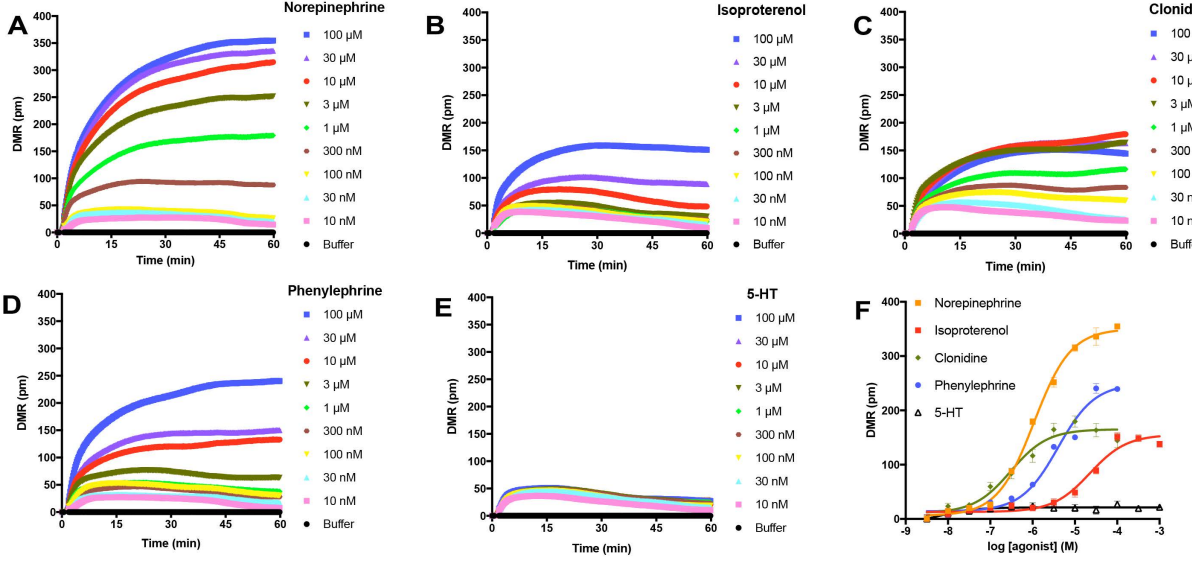
A
Norepinephrine
B
Isoproterenol
C
Clonidine
D
Phenylephrine
E
5-HT
F
100 µM
30 µM
10 µM
3 µM
1 µM
300 nM
100 nM
30 nM
10 nM
Buffer
DMR (pm)
Time (min)
log [agonist] (M)

Fig. 2.

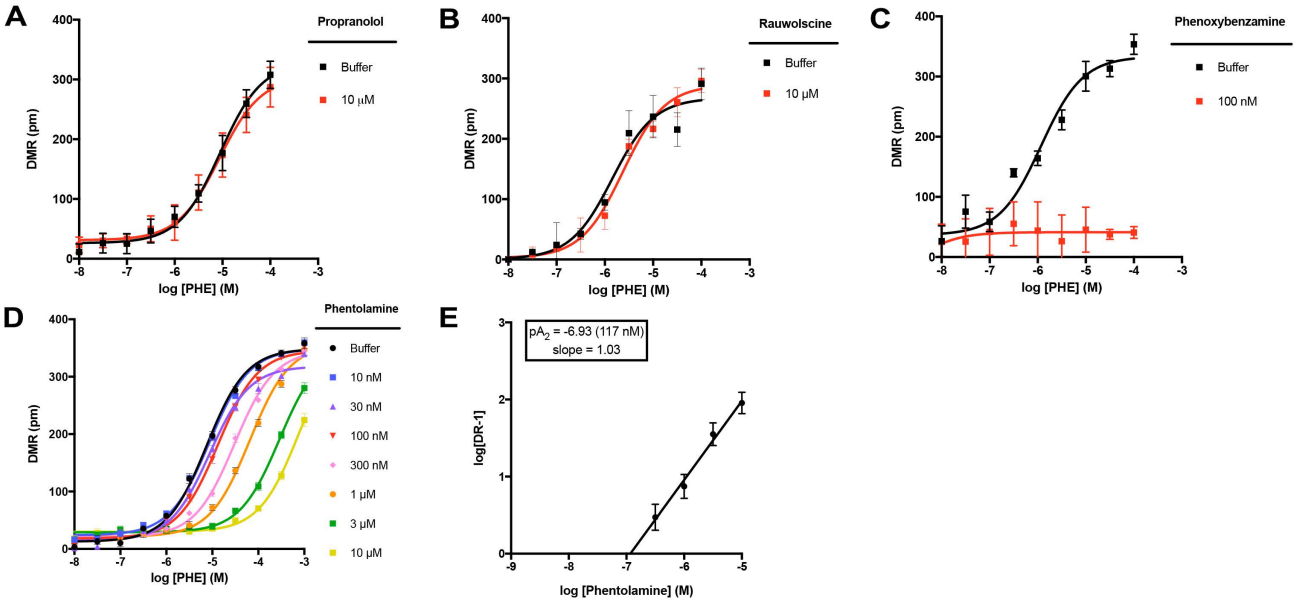
A
Propranolol
Buffer
10 μM
DMR (pm)
log [PHE] (M)
B
Rauwolscine
Buffer
10 μM
DMR (pm)
log [PHE] (M)
C
Phenoxybenzamine
Buffer
100 nM
DMR (pm)
log [PHE] (M)
D
Phentolamine
Buffer
10 nM
30 nM
100 nM
300 nM
1 μM
3 μM
10 μM
DMR (pm)
log [PHE] (M)
E
pA2 = -6.93 (117 nM)
slope = 1.03
log[DR-1]
log [Phentolamine] (M)

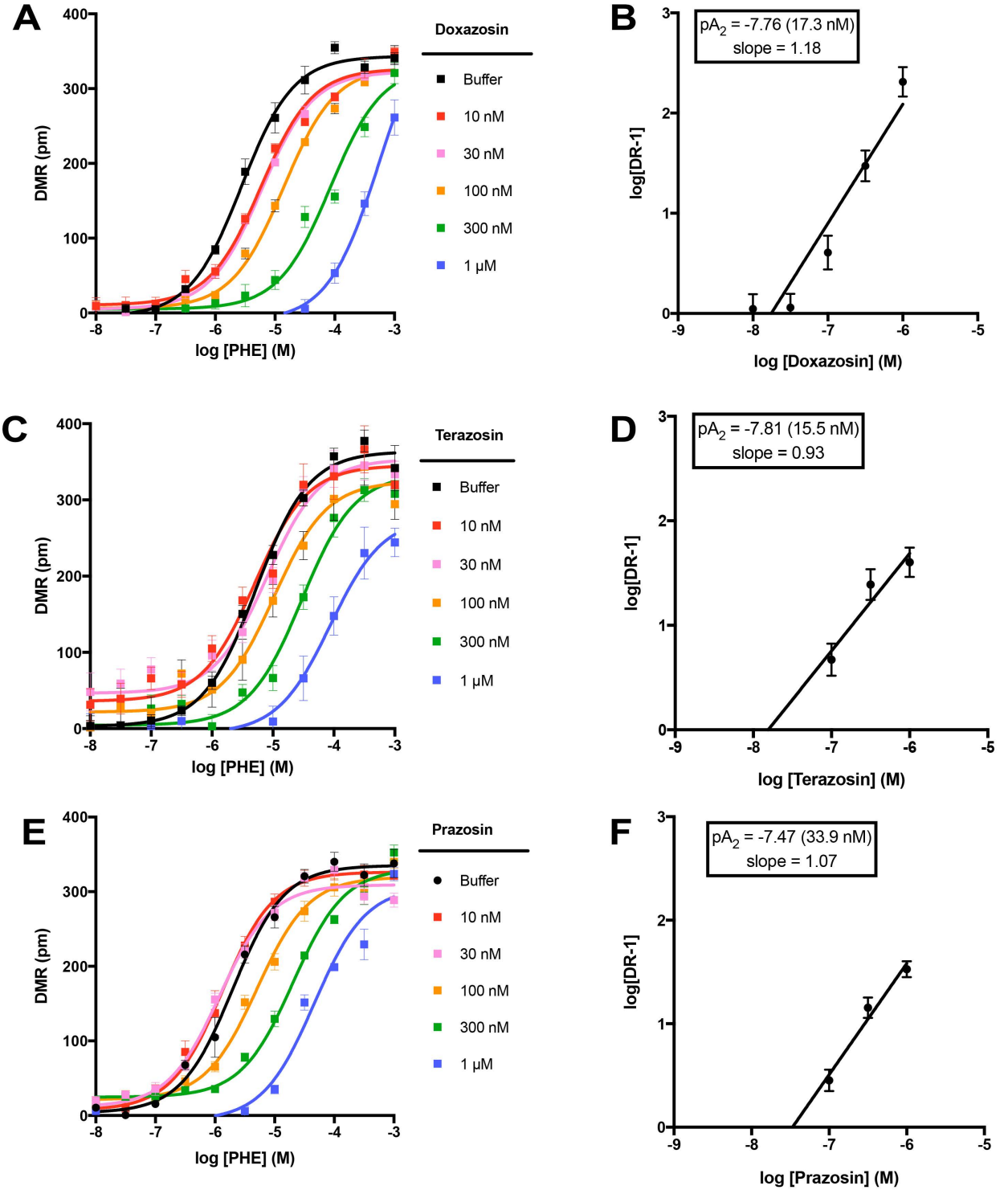
A
DMR (pm)
log [PHE] (M)
Doxazosin
Buffer
10 nM
30 nM
100 nM
300 nM
1 μM
B
pA2 = -7.76 (17.3 nM)
slope = 1.18
log[DR-1]
log [Doxazosin] (M)
C
DMR (pm)
log [PHE] (M)
Terazosin
Buffer
10 nM
30 nM
100 nM
300 nM
1 μM
D
pA2 = -7.81 (15.5 nM)
slope = 0.93
log[DR-1]
log [Terazosin] (M)
E
DMR (pm)
log [PHE] (M)
Prazosin
Buffer
10 nM
30 nM
100 nM
300 nM
1 μM
F
pA2 = -7.47 (33.9 nM)
slope = 1.07
log[DR-1]
log [Prazosin] (M)

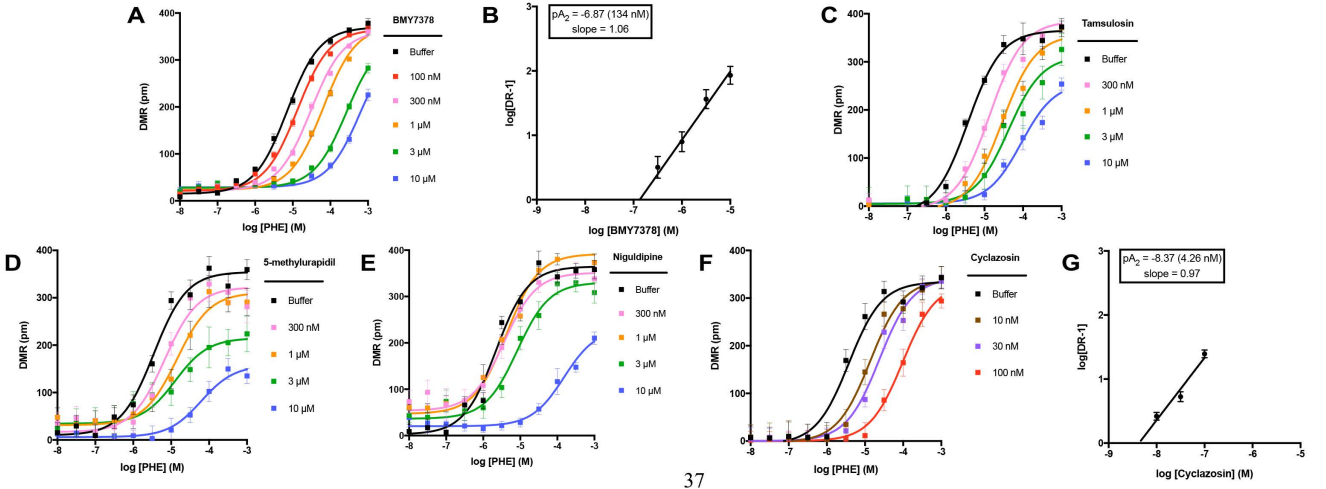
A
DMR (pm)
log [PHE] (M)
BMY7378
Buffer
100 nM
300 nM
1 µM
3 µM
10 µM
B
pA2 = -6.87 (134 nM)
slope = 1.06
log[DR-1]
log [BMY7378] (M)
C
DMR (pm)
log [PHE] (M)
Tamsulosin
Buffer
300 nM
1 µM
3 µM
10 µM
D
DMR (pm)
log [PHE] (M)
5-methylurapidil
Buffer
300 nM
1 µM
3 µM
10 µM
E
DMR (pm)
log [PHE] (M)
Nigulidipine
Buffer
300 nM
1 µM
3 µM
10 µM
F
DMR (pm)
log [PHE] (M)
Cyclazosin
Buffer
10 nM
30 nM
100 nM
G
pA2 = -8.37 (4.26 nM)
slope = 0.97
log[DR-1]
log [Cyclazosin] (M)

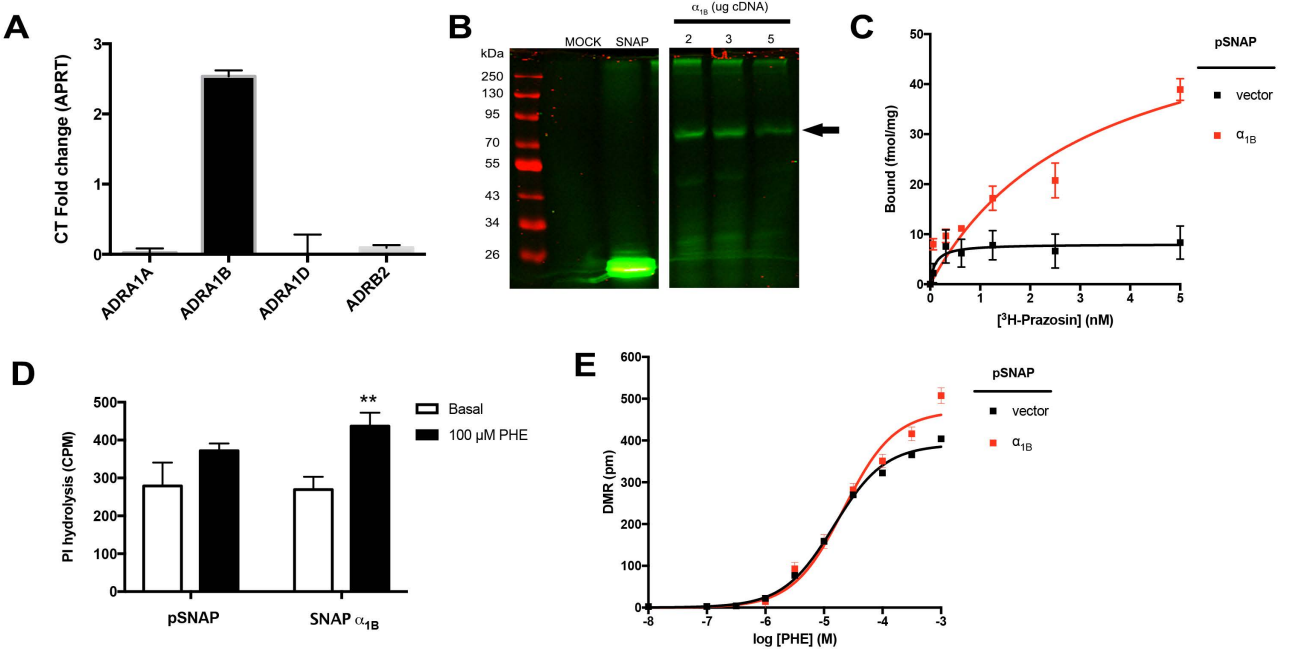
A
CT Fold change (APRT)
ADRA1A
ADRA1B
ADRA1D
ADRB2
B
MOCK
SNAP
α1B (ug cDNA)
2
3
5
kDa
250
130
95
70
55
43
34
26
C
pSNAP
vector
α1B
Bound (fmol/mg)
[3H-Prazosin] (nM)
D
Basal
100 μM PHE
PI hydrolysis (CPM)
**
pSNAP
SNAP α1B
E
pSNAP
vector
α1B
DMR (pm)
log [PHE] (M)

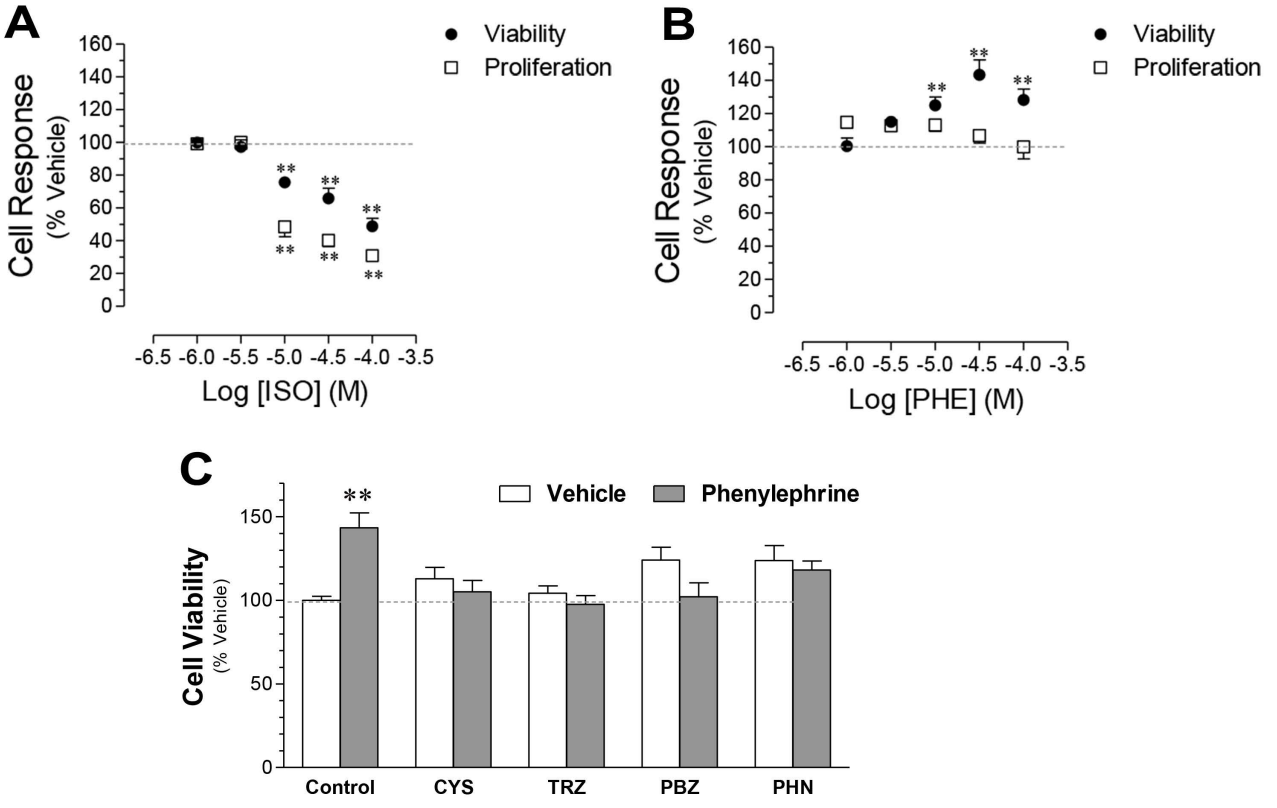
A
Cell Response
(% Vehicle)
160
140
120
100
80
60
40
20
0
Viability
Proliferation
**
-6.5 -6.0 -5.5 -5.0 -4.5 -4.0 -3.5
Log [ISO] (M)
B
Cell Response
(% Vehicle)
Viability
Proliferation
**
-6.5 -6.0 -5.5 -5.0 -4.5 -4.0 -3.5
Log [PHE] (M)
C
Cell Viability
(% Vehicle)
150
100
50
0
**
Vehicle
Phenylephrine
Control
CYS
TRZ
PBZ
PHN

Label-free dynamic mass redistribution reveals low density, pro-survival α_{1B}-adrenergic receptors in human SW480 colon carcinoma cells

Journal of Pharmacology and Experimental Therapeutics

Dorathy-Ann Harris, Ji-Min Park, Kyung-Soon Lee, Cong Xu, Nephi Stella and Chris Hague

Supplemental Figure 1

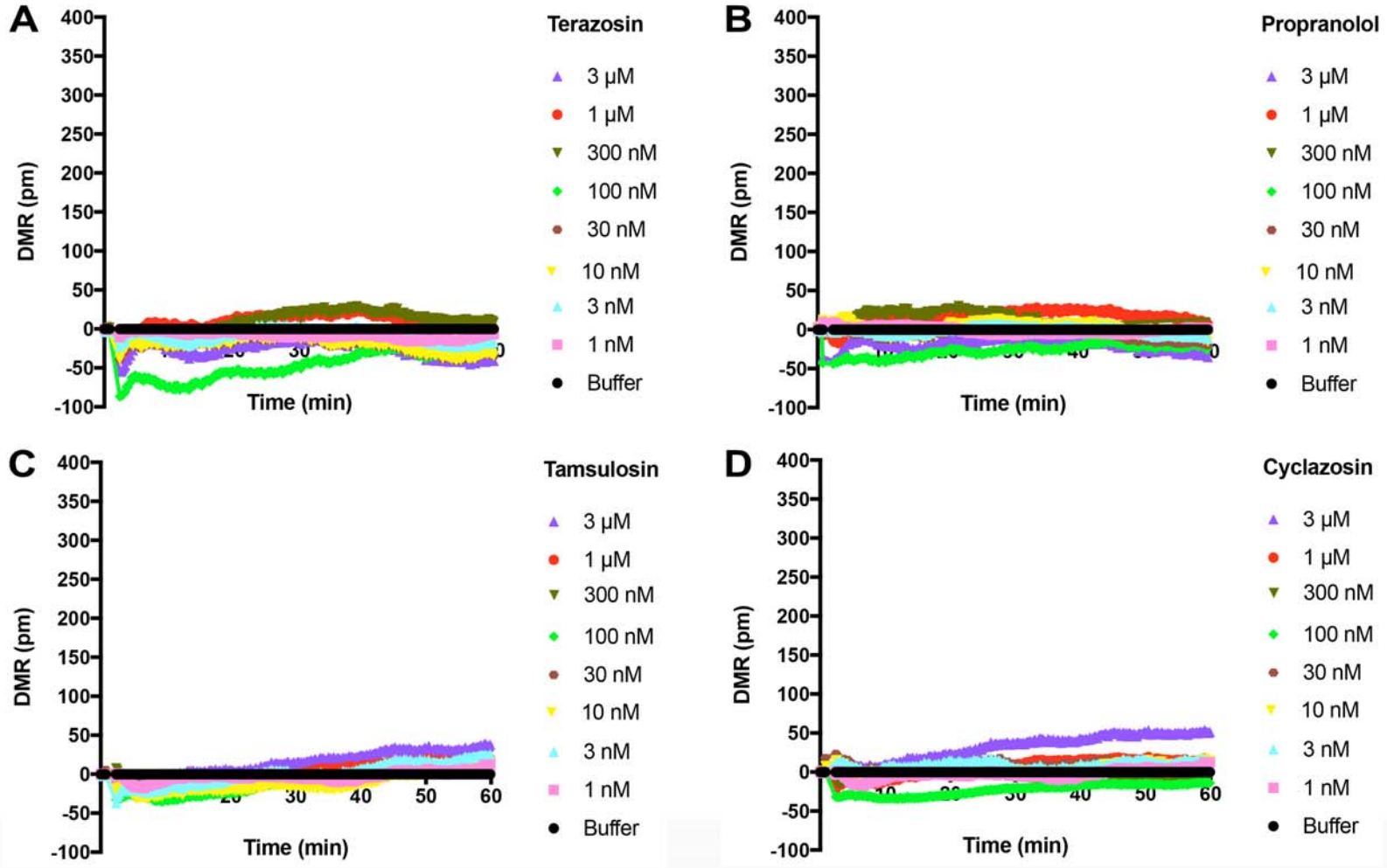

Supplemental Figure 1. Adrenergic receptor (AR) antagonist dynamic mass redistribution responses in human SW480 colon carcinoma cells. Raw label-free dynamic mass redistribution responses were measured for the α_1-AR antagonist terazosin (A), the β-AR antagonist propranolol (B), the $\alpha_{1A/D}$-AR selective antagonist tamsulosin (C), or the α_{1B}-AR selective antagonist cyclazosin (D). Data are mean of 2 independent experiments performed with 4 replicates.